A Transactive Energy Framework for Inverter-based HVAC Loads in a Real-time Local Electricity Market Considering Distributed Energy Resources

Hongxun Hui, *Member, IEEE*, Pierluigi Siano, *Senior Member, IEEE*, Yi Ding, *Member, IEEE*, Peipei Yu, Yonghua Song, *Fellow, IEEE*, Hongcai Zhang, *Member, IEEE*, and Ningyi Dai, *Member, IEEE*

***Abstract*—Rapidly increasing distributed energy resources (DERs) bring more fluctuating output power to the distribution network and put forward a higher requirement on local regulation resources for maintaining the network's balance. Heating, ventilation, and air conditioning (HVAC) loads account for more than 40% of power consumption in modern cities and have huge regulation potential as flexible loads. However, HVACs equipped with inverter devices have rarely been studied for providing regulation services in the local electricity market (LEM), even though they have exceeded regular fixed-speed HVACs. To address this issue, this paper proposes a real-time LEM and a distribution network's optimization framework to exploit the regulation potential of inverter-based HVACs considering multiple DERs. This LEM can avoid iterations in real-time and significantly decrease the difficulty related to the participation of small end-users in urban distribution networks. Moreover, we propose a transactive capacity evaluation method to assist end-users in deciding their inverter-based HVACs' regulation capacities in the real-time LEM, which considers buildings' thermal features, users' multiple comfort requirements, and dynamic ambient temperature. On this basis, a multi-level bidding strategy is developed for inverter-based HVACs to decrease energy cost, increase fluctuating DERs' local utilization rate, and alleviate the distribution network's congestion. Finally, a realistic distribution network is utilized to verify the effectiveness of the proposed methods.**

***Index Terms*—Local electricity market, inverter-based HVAC loads, transactive energy, distributed energy resources.**

I. Introduction

THE rapidly increasing distributed energy resources (DERs), such as photovoltaics (PVs) and wind turbines, are transforming urban distribution networks from pure consumers into prosumers [1]. More and more urban distribution networks can not only import but also export electricity to the main grid, especially during the DERs' peak generation periods [2]. However, differently from traditional generating units (e.g., thermal power units), DERs' output power is seriously affected by the environment with great uncertainties [3], which causes the tie-line power between the main grid and distribution networks to become more fluctuating. The main grid has to reserve more flexible regulation resources for maintaining the system balance, which undoubtedly decreases the system's economic efficiency [4]. More seriously, with the phasing out of traditional generating units (main contributors of regulation resources nowadays), the regulation resources in the system will probably be insufficient. This is one of the main threats to the power system's stable and secure operation [5].

To address this issue, more studies are paying attention to demand side regulation resources [6] and the local electricity market (LEM) for transactive energy in distribution networks [7]. For example, Daneshvar et al. [8] develop a two-stage robust stochastic scheduling model considering the transactive energy in day-ahead and real-time markets, which can enable the distribution networks with high-penetration DERs to participate in the deregulated market effectively [9]. Nunna et al. [10] and Nizami et al. [11] propose multiagent-based transactive energy frameworks for distribution networks to integrate demand side regulation resources into the system operation. Lin et al. [12] analyze different auction mechanisms and bidding strategies for DERs' transactive energy market. Rayati et al. [13] develop a resilient transactive control method for high wind penetration systems based on cloud computing. Hu et al. [14] propose a balancing market framework by adopting the concept of network-constrained transactive energy to facilitate the interactions between the transmission system and DERs [15]. Li et al. [16] integrate a bilateral energy trading mechanism with the optimal power flow technique to increase participants' benefits. Moreover, multi-microgrid systems with transactive energy are optimized by second-order cone programming [17], Karush-Kuhn-Tucker optimality conditions [18], distributionally robust optimization [19], and scenario-based stochastic optimization method [20]. Some decentralized schemes are also designed. For example, Yang et al. [21] develop a blockchain-empowered socially optimal transactive energy system to guarantee the users' benefits while avoiding privacy data leakage [22]. Yan et al. [23] propose network-constrained peer-to-peer transactive energy for microgrids, which can guarantee the distribution network security and increase transaction flexibility [24]. Jhala et

Manuscript received June 29, 2021; revised December 25, 2021, and accepted February 04, 2022. This work is supported in part by the National Science Foundation for Distinguished Young Scholars of China under Grant 52125702, and the Science and Technology Development Fund, Macau SAR (File no. SKL-IOTSC(UM)-2021-2023, File no. 0003/2020/AKP). Paper no. TII-21-2710. (Corresponding authors: *Pierluigi Siano; Yi Ding.*)

H. Hui, P. Yu, Y. Song, H. Zhang, and N. Dai are with the State Key Laboratory of Internet of Things for Smart City and the Department of Electrical and Computer Engineering, University of Macau, Macau 999078, China (e-mails: hongxunhui@um.edu.mo; yc07431@connect.um.edu.mo; yhsong@um.edu.mo; hczhang@um.edu.mo; nydai@um.edu.mo).

P. Siano is with the Department of Management & Innovation Systems, University of Salerno, Salerno 84084, Italy (e-mail: psiano@unisa.it).

Y. Ding is with the College of Electrical Engineering, Zhejiang University, Hangzhou 310027, China (yiding@zju.edu.cn).

Color versions of one or more of the figures in this paper are available online at http://ieeexplore.ieee.org.

al. [25] analyze the impact of attacks on pricing signals in the transactive energy market to highlight the concern for false data injection [26]. Feng et al. [27] propose a coalitional game model to utilize flexible loads and fluctuating power of DERs.

Among different kinds of demand side regulation resources, battery storage systems are especially concerned [29], which can be installed along with distributed DERs to mitigate their intermittent output power [30]. However, the installed capacity of batteries is still small and the cost is relatively high, more attention has been paid to flexible loads [31], [32]. Heating, ventilation, and air conditioning (HVAC) is one of the most important flexible loads in urban distribution networks [33], since they account for a large proportion of the total power consumption (e.g., more than 40% in many cities around the world) and thus have a huge regulation potential [34]. Also, the indoor temperature can be guaranteed in comfortable ranges during the regulation process by utilizing buildings' thermal storage characteristics [35]. Therefore, HVACs are suitable to be controlled as flexible regulation resources [36]. Liu et al. [37] propose a deep reinforcement learning algorithm to achieve the optimal and automated control of HVACs, which can balance the electricity costs and users' comforts. Mohammad et al. [38] develop a transactive control method for HVACs to modify the operating power at peak hours. Behboodi et al. [39] propose a market-based transactive control method for HVACs to achieve fast-acting to real-time retail electricity prices. Moreover, Shen et al. [40] design a two-tier transactive control scheme for real-time congestion management in distribution networks. Pinto et al. [41] propose a decision support model to optimize small players' negotiations in multiple alternative market opportunities. However, the existing studies still have some drawbacks on the regulation of HVACs in the real-time LEM, mainly in the following three aspects:

1) Most existing studies focus on regular fixed-speed HVACs, whose compressors can only operate in two modes (i.e., ON and OFF) to adjust the indoor temperature, as shown in Fig. 1(a) [42]. Note that this paper assumes the HVAC operates in a cooling state in summer. When the indoor temperature reaches the upper limit of the user's set temperature, the HVAC is switched ON. By contrast, when the indoor temperature reaches the lower limit of the set temperature, the HVAC is switched OFF [43]. Therefore, the power consumption of regular fixed-speed HVACs can only be switched between the rated power $P^{\text{rate}}_{\text{HVAC},i}$ and zero power [44]. Furthermore, one HVAC only has one regulation direction at any time, i.e., its power can only be reduced to zero when the HVAC is operating in ON-mode (i.e., $P^{\text{down}}_{\text{HVAC},i}$ in Fig. 1(a)); its power can only be increased to the rated value when the HVAC is operating in OFF-mode (i.e., $P^{\text{up}}_{\text{HVAC},i}$ in Fig. 1(a)). This is unfavorable for the flexible control of HVACs in the real-time LEM. Apart from this kind of regular fixed speed HVACs, HVACs with inverter devices can change their operating power continuously and flexibly, as shown in Fig. 1(b). Based on the market analysis report [45], the market share of inverter-based HVACs is expanding rapidly and has exceeded the share of regular fixed speed HVACs. Therefore, inverter-based HVACs have a huge regulation potential and are suitable to participate in the real-time LEM [46], while there are few targeted studies on the transactive control of inverter-based HVACs in real-time LEM.

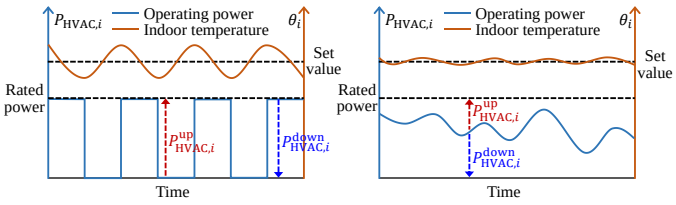

(a) Regular fixed speed HVAC. (b) Continuously adjustable HVAC.

Fig. 1. The HVAC's operating power and corresponding indoor temperature.

2) Most existing studies assume that HVACs' users can submit the transactive capacities to the market by themselves, i.e., the available decreasing or increasing quantities of HVACs' power consumption [47]-[48]. However, in reality, small end-users (e.g., residential users and small commercial users) have no professional knowledge or ability to quote the transactive capacity. Most of the small end-users do not even know the power consumption of various appliances at a different time in a day, and surely cannot submit their transactive capacities to the real-time LEM. Furthermore, compared with the constant regulation capacity from regular fixed speed HVACs (i.e., $P^{\text{down}}_{\text{HVAC},i} = P^{\text{up}}_{\text{HVAC},i} = P^{\text{rate}}_{\text{HVAC},i}$ in Fig. 1(a)), the transactive capacity evaluation of the inverter-based HVAC (i.e., $P^{\text{up}}_{\text{HVAC},i}$ and $P^{\text{down}}_{\text{HVAC},i}$ in Fig. 1(b)) is more complex because the inverter-based HVAC's operating power $P^{\text{operate}}_{\text{HVAC},i}(t)$ is related to variable surroundings, including the real-time indoor temperature, the user's set temperature and the ambient temperature. To complicate matters further, even though we can monitor the i-th inverter-based HVAC's operating power $P^{\text{operate}}_{\text{HVAC},i}(t)$ and obtain its transactive capacities as follows:

$$\begin{cases} P^{\text{up}}_{\text{HVAC},i}(t) = P^{\text{rate}}_{\text{HVAC},i} - P^{\text{operate}}_{\text{HVAC},i}(t), & \forall i \in \mathcal{I}, \forall t \in \mathcal{T}, \\ P^{\text{down}}_{\text{HVAC},i}(t) = P^{\text{operate}}_{\text{HVAC},i}(t), & \forall i \in \mathcal{I}, \forall t \in \mathcal{T}, \end{cases} \tag{1}$$

where $\mathcal{I}$ and $\mathcal{T}$ are the set of HVACs and time slots, respectively. Symbols $P^{\text{up}}_{\text{HVAC},i}(t)$ and $P^{\text{down}}_{\text{HVAC},i}(t)$ are the maximum up and down adjustable capacities, respectively. These two values are calculated purely from a physical perspective, and cannot be regarded as the available transactive capacities of the inverter-based HVACs, because the user's comfort requirement on the indoor temperature during the regulation process is not considered in these maximum adjustable capacities. That is to say, when the regulation duration time, the user's comfort constraints and uncertain surroundings are considered. The actual available transactive capacities of inverter-based HVACs probably become smaller than the values calculated in Eq. (1). According to the social-behavioural survey on load regulation projects in New York and Texas in the U.S. [49], both the comfort and benefit in the market are the main concerns of electricity users. Therefore, to make the inverter-based HVAC's regulation executable in reality, the up-and down-regulation capacities should be evaluated comprehensively to fully utilize the HVAC's regulation potential to improve users' benefit while maintaining users' comfort all the time. To the best of our knowledge, there is no targeted research on the intelligent transactive capacity evaluation method of inverter-based HVACs for participating in the real-time LEM.

3) Many existing studies on LEM are based on the iterative bidding framework to achieve the global optimum (e.g., maximizing the system profit or minimizing the system cost) [50]-[53]. The general process is as follows: first, the distribution system operator (DSO) collects the participants' quoting prices in the distribution network, such as the transactive capacities and bidding prices from end-users, and the power generation capacities and offer prices from DERs. Then these data are packaged and submitted to the wholesale market, where the independent system operator (ISO) can clear the system's electricity price. Based on the clearing electricity price from the main grid, the DSO re-optimizes the prices in the LEM for maximizing its profit or minimizing the distribution network's cost. These updated prices are then broadcast to the participants in the LEM, and each participant submits its quoting information again. This iterative process will end until the DSO's profit does not increase or the distribution network's cost does not decrease. However, in reality, small end-users of inverter-based HVACs cannot be on call day and night to submit their transactive capacities. This causes many studies on load regulation to be hard to implement extensively in practice.

To fill the above research gaps, the main contributions of this paper can be summarized as follows:

1) A real-time LEM is proposed considering multiple participants, including inverter-based HVACs, PVs, wind turbines, and diesel generators. This real-time LEM avoids the need for iterations to decrease the participation difficulty for small end-users.
2) A transactive capacity evaluation method of inverter-based HVACs in the real-time LEM is proposed, which considers the regulation duration time, the dynamic ambient temperature, the building's heat conduction, the air ventilation, and the user's multiple comfort requirements.
3) A multi-level bidding method for the inverter-based HVAC is designed based on its transactive capacity and historical distribution locational marginal prices (D-LMPs), which achieves the decrease of user's energy cost, the increase of DERs' local utilization rate, and the alleviation of distribution network's power congestion.

The remainder of this paper is organized as follows. Section II presents the framework and the optimization model of the real-time LEM. Section III shows the transactive capacity evaluation method and the multi-level bidding strategy of inverter-based HVACs. Numerical studies are presented in Section IV. Section V concludes this paper.

II. The Real-time Local Electricity Market

A. The Framework of the Real-time LEM

The framework of the real-time LEM is shown in Fig. 2. From the topology perspective, each distribution network is connected with the main grid through the tie-line. In this manner, the distribution network can import/export electricity from/to the main grid. From the system operator perspective, the ISO is responsible for clearing the wholesale market and maintaining the main grid balance. The DSO is in charge of clearing the LEM to optimize the distribution network.

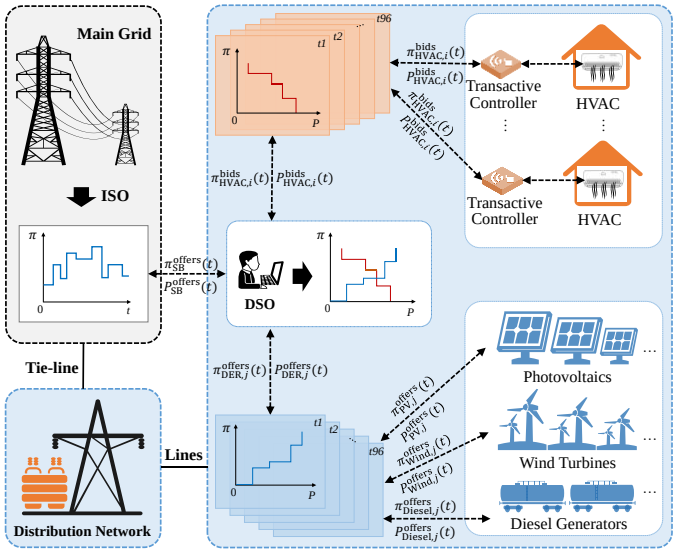

Fig. 2. The framework of the real-time LEM considering multiple DERs and inverter-based HVACs.

In the distribution network, the DERs include PVs, wind turbines, and diesel generators. The loads are divided into two categories: conventional unchangeable loads and adjustable loads. Specifically, in this paper, inverter-based HVACs are considered as adjustable loads due to the flexible regulation characteristic and huge power consumption share in realistic power systems. Therefore, the participants in the real-time LEM can be summarized as follows: the main grid, PVs, wind turbines, diesel generators, and inverter-based HVACs.

B. Optimization Model of the Real-time LEM

The time slot of the real-time LEM is assumed to be 15min (i.e., $\mathcal{T}=\{t \mid t=1,2,\cdots,96\}$ for one day). In the pre-operating slot (i.e, 15min earlier), all the participants submit their active energy bids and offers to the DSO in block forms. As shown in Fig. 2, on the demand side, loads submit the bidding prices $\pi_{\mathrm{D},i}^{\mathrm{bids}}(t)$ and energies $P_{\mathrm{D},i}^{\mathrm{bids}}(t)$; on the supply side, DERs (including PVs, wind turbines, and diesel generators) offer the output energy quantities $P_{\mathrm{DER},j}^{\mathrm{offers}}(t)$ and prices $\pi_{\mathrm{DER},j}^{\mathrm{offers}}(t)$ to the DSO. Considering this paper mainly pays attention to the energy trading within the distribution network, the DSO is assumed to be a price-taker from the ISO (i.e., $\pi_{\mathrm{SB}}^{\mathrm{offers}}(t)$ in Fig. 2). Based on the above bids and offers from all the participants, the DSO can clear the D-LMPs and active energy quantities at each distribution network's bus [54]. The objective of the optimization model is to maximize the social welfare. As shown in Fig. 3, the social welfare is defined as the total benefits on the demand side minus the total costs on the supply side. Hence, the objective function can be expressed as:

$$\mathrm{Max} \quad \left[\sum_{i=1}^{I} B_i(P_{\mathrm{D},i}^{\mathrm{bids}}, \pi_{\mathrm{D},i}^{\mathrm{bids}}) - \sum_{j=1}^{J} C_j(P_{\mathrm{S},j}^{\mathrm{offers}}, \pi_{\mathrm{S},j}^{\mathrm{offers}})\right], \quad \forall i \in \mathcal{I},\ \forall j \in \mathcal{J}, \tag{2}$$

where $\mathcal{I}=\{i \mid i=1,2,\cdots,I\}$ and $\mathcal{J}=\{j \mid j=1,2,\cdots,J\}$ are the set of participants on demand and supply sides, respectively. Symbols B_i and C_j are the *i*-th participant's benefit on demand side and the *j*-th participant's cost on supply-side, respectively. As shown in Fig. 3, each block means the available

energy and the corresponding price of one DER or some DERs (because some DERs may have the same bidding prices). Just like most electricity markets around the world, the prices from distributed PVs and winds are set as zero. The prices from diesel generators and the main grid increase with the increase of the offered energy. Based on the above bids and offers from all the participants, the DSO can clear the D-LMPs and active energy quantities at each distribution network's bus.

The optimization model is subject to the power balance constraint at each bus, which is expressed as:

$$\begin{cases} P_k^{\mathrm{G}} - P_k^{\mathrm{L}} = \sum_{l=1}^{N_{\mathrm{bus}}} V_k V_l \left[G_{kl} \cos(\theta_k - \theta_l) + B_{kl} \sin(\theta_k - \theta_l) \right], \\ Q_k^{\mathrm{G}} - Q_k^{\mathrm{L}} = \sum_{l=1}^{N_{\mathrm{bus}}} V_k V_l \left[G_{kl} \sin(\theta_k - \theta_l) + B_{kl} \cos(\theta_k - \theta_l) \right], \\ \forall (k,l) \in \mathcal{N}_{\mathrm{bus}}, \end{cases} \tag{3}$$

where P_k^{G} and P_k^{L} are the generated and absorbed active power at the *k*-th bus, respectively; V_k and V_l are voltage magnitude at the *k*-th and *l*-th bus, respectively; G_{kl} and B_{kl} are the element's real part and imaginary part of the bus admittance matrix, respectively; θ_k and θ_l are the voltage angles at the *k*-th and *l*-th bus, respectively; Q_k^{G} and Q_k^{L} are the generated and absorbed reactive power at the *k*-th bus, respectively; $\mathcal{N}_{\mathrm{bus}}$ is the set of the distribution network's buses.

Moreover, the optimization model is subject to some inequality constraints, including:

$$P_{\mathrm{SB}}^{\min} \le P_{\mathrm{SB}} \le P_{\mathrm{SB}}^{\max}, \tag{4}$$

$$Q_{\mathrm{SB}}^{\min} \le Q_{\mathrm{SB}} \le Q_{\mathrm{SB}}^{\max}, \tag{5}$$

$$V_k^{\min} \le V_k \le V_k^{\max}, \ \forall k \in \mathcal{N}_{\mathrm{bus}}, \tag{6}$$

$$S_h - S_h^{\max} \le 0, \ \forall h \in \mathcal{N}_{\mathrm{line}}, \tag{7}$$

$$0 \le P_{\mathrm{DER},j}^{\mathrm{offers}} \le P_{\mathrm{DER},j}^{\mathrm{offers,max}}, \ \forall j \in \mathcal{J}, \tag{8}$$

$$\cos\varphi_{\mathrm{DER},j} = P_{\mathrm{DER},j}^{\mathrm{offers}} \Big/ \sqrt{(P_{\mathrm{DER},j}^{\mathrm{offers}})^2 + (Q_{\mathrm{DER},j}^{\mathrm{offers}})^2}, \ \forall j \in \mathcal{J}, \tag{9}$$

$$P_{\mathrm{DER},j}^{\mathrm{offers}}(t) - P_{\mathrm{DER},j}^{\mathrm{offers}}(t-1) \le UR_{\mathrm{DER},j}, \ \forall j \in \mathcal{J}, \tag{10}$$

$$P_{\mathrm{DER},j}^{\mathrm{offers}}(t-1) - P_{\mathrm{DER},j}^{\mathrm{offers}}(t) \le DR_{\mathrm{DER},j}, \ \forall j \in \mathcal{J}, \tag{11}$$

$$P_{\mathrm{D},i}^{\mathrm{bids,min}} \le P_{\mathrm{D},i}^{\mathrm{bids}} \le P_{\mathrm{D},i}^{\mathrm{bids,max}}, \ \forall i \in \mathcal{I}, \tag{12}$$

where Eqs. (4)-(5) are constraints of the active power P_{SB} and reactive power Q_{SB} on the slack bus (i.e., the interconnection bus between the distribution network and the main grid), respectively. The superscripts $(\cdot)^{\min}$ and $(\cdot)^{\max}$ indicate the minimum and maximum values of the quantity, respectively. Eq. (6) is the constraint of the voltage magnitude V_k at the *k*-th bus. Eq. (7) indicates the constraint of the apparent power transfer S_h at the *h*-th line. In this paper, the maximum line's capacities $S_h^{\max}$ are regarded as hard constraints of the optimization. Eqs. (8) and (9) are the *j*-th DER's active power $P_{\mathrm{DER},j}^{\mathrm{offers}}$ and reactive power $Q_{\mathrm{DER},j}^{\mathrm{offers}}$ constraints, respectively, where DERs are assumed to operate at a constant power factor $\cos\varphi_{\mathrm{DER},j}$. Eqs. (10) and (11) are the constraints of the *j*-th DER's ramp rates, in which $UR_{\mathrm{DER},j}$ and $DR_{\mathrm{DER},j}$ are the ramp-up and ramp-down rate limits of the *j*-th DER, respectively. Eq. (12) is the *i*-th load's operating power constraints.

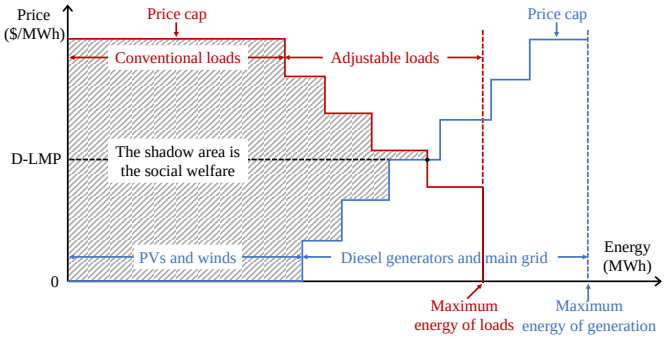

Fig. 3. The bidding blocks of DERs and loads to maximize the social welfare.

Generally, the distribution network's constraints in Eqs. (4)-(7) and the DERs' constraints in Eqs. (8)-(11) are fixed or can be predicted by some off-the-shelf methods [55]. By contrast, the available regulation capacity constraints of loads in Eqs. (12) are complex. As for inverter HVACs, the values $P_{\mathrm{HVAC},i}^{\mathrm{bids,min}}$ and $P_{\mathrm{HVAC},i}^{\mathrm{bids,max}}$ are related to many changeable factors, including the real-time LEM's regulation duration time (e.g., 15min), the user's comfort constraints (e.g., the maximum indoor temperature deviation is 1ºC), the variable ambient temperature, the building's heat conduction, and the building's ventilation rate. Therefore, the evaluation method considering multiple factors is one of the key problems for promoting inverter-based HVACs to participate in the real-time LEM, which is presented in the following Section III.

III. Transactive Capacity Evaluation and Multi-level Bidding Strategy of Inverter-Based HVACs

A. Modelling of Inverter-based HVAC

To study the operating characteristic and power consumption of the inverter-based HVAC, the corresponding building's thermal model should be developed, which can be expressed as:

$$\begin{aligned} & C_i \frac{d\theta_i(t)}{dt} = H_{\mathrm{Cond},i}(t) + H_{\mathrm{Vent},i}(t) - H_{\mathrm{HVAC},i}(t), \\ & \forall i \in \mathcal{I}, \forall t \in \mathcal{T}, \end{aligned} \tag{13}$$

where C_i is the building's thermal capacity; θ_i is the indoor temperature; $H_{\mathrm{HVAC},i}$ is the cooling capacity from the inverter-based HVAC. Symbols $H_{\mathrm{Cond},i}$ and $H_{\mathrm{Vent},i}$ indicate the heat gains through conduction and ventilation, respectively, which can be calculated as:

$$\begin{cases} H_{\mathrm{Cond},i}(t) = (\theta_o(t) - \theta_i(t)) \big/ R_i, & \forall i \in \mathcal{I}, \forall t \in \mathcal{T}, \\ H_{\mathrm{Vent},i}(t) = C_i \nu_i(t) (\theta_o(t) - \theta_i(t)), & \forall i \in \mathcal{I}, \forall t \in \mathcal{T}, \end{cases} \tag{14}$$

where θ_o is the ambient temperature; R_i is the building's thermal resistance; ν_i is the building's ventilation rate.

The inverter-based HVAC's cooling capacity depends on its operating power, whose relationship can be expressed as:

$$H_{\mathrm{HVAC},i}(t) = \eta_i \cdot P_{\mathrm{HVAC},i}(t), \ \forall i \in \mathcal{I}, \forall t \in \mathcal{T}, \tag{15}$$

where η_i is the energy efficiency ratio; $P_{\mathrm{HVAC},i}$ is the inverter-based HVAC's operating power, which can be flexibly regulated by adjusting the compressor's rotating frequency:

$$P_{\mathrm{HVAC},i}(t) = \xi_i f_i(t) + \sigma_i, \ \forall i \in \mathcal{I}, \forall t \in \mathcal{T}, \tag{16}$$

where f_i is the compressor's rotating frequency; symbols ξ_i

and σ_i are coefficients of the operating power and compressor's rotating frequency.

B. Transactive Capacity Evaluation of Inverter-based HAVC

Based on Eqs. (13)-(15), we know that the indoor temperature θ_i will be affected when the inverter-based HVAC adjusts its operating power $P_{\mathrm{HVAC},i}$. In the real-time LEM, if we want to guarantee the user's comfort constraint during the regulation process, the relationship between the indoor temperature deviation $\Delta\theta_i$ and the adjustment value of the operating power $\Delta P_{\mathrm{HVAC},i}$ should be derived considering multiple changeable factors, such as the ambient temperature θ_o, the ventilation rate ν_i, and the regulation duration time T_{D}. To address this issue, we can substitute Eqs. (14)-(15) into Eq. (13) and get:

$$\begin{cases} C_i \dfrac{d\theta_i(t)}{dt} = \gamma_i(t)\cdot(\theta_o(t)-\theta_i(t)) - \eta_i P_{\mathrm{HVAC},i}(t), \\ \gamma_i(t) = (1+R_i C_i \nu_i(t))/R_i, \quad \forall i \in \mathcal{I}, \forall t \in \mathcal{T}. \end{cases} \tag{17}$$

where $\gamma_i(t)$ is the equivalent heat transfer coefficient of the i-th building. It is assumed that the regulation begins at time t_{I} and ends at the time t_{II} (i.e., the regulation duration time $T_{\mathrm{D}} = t_{\mathrm{II}} - t_{\mathrm{I}}$). Then we can solve the definite integral of both sides in Eq. (17):

$$\begin{aligned} &\int_{t_{\mathrm{I}}}^{t_{\mathrm{II}}} C_i d\theta_i(t) = \int_{t_{\mathrm{I}}}^{t_{\mathrm{II}}} [\gamma_i(t)(\theta_o(t)-\theta_i(t)) - \eta_i P_{\mathrm{HVAC},i}(t)]dt, \\ \Leftrightarrow\ & C_i(\theta_i^{\mathrm{II}} - \theta_i^{\mathrm{I}}) = \int_{t_{\mathrm{I}}}^{t_{\mathrm{II}}} \gamma_i(t)\theta_o(t)dt - \int_{t_{\mathrm{I}}}^{t_{\mathrm{II}}} \gamma_i(t)\theta_i(t)dt \\ &\qquad - \int_{t_{\mathrm{I}}}^{t_{\mathrm{II}}} \eta_i P_{\mathrm{HVAC},i}(t)dt, \ \forall i \in \mathcal{I}, \forall t \in \mathcal{T}. \end{aligned} \tag{18}$$

where θ_i^{I} and θ_i^{II} are the indoor temperatures at the time t_{I} and t_{II}, respectively.

Note that the inverter-based HVAC's operating power can be regulated both up and down based on the bidding results in the real-time LEM. Therefore, the indoor temperature deviation during the regulation process (i.e., $\Delta\theta_i = \theta_i^{\mathrm{II}} - \theta_i^{\mathrm{I}}$) can be positive and negative values in down- and up-regulation conditions, respectively. It is assumed that the inverter-based HVACs in this paper operate in a cooling state in summer. Then the relationship between the operating power regulation capacities and the indoor temperature deviations are shown in Fig. 4. The indoor temperature will be decreased after raising the operating power, and vice versa. During the regulation process in a one-time slot, the inverter-based HVAC's operating power $P^{\mathrm{reg}}_{\mathrm{HVAC},i}$ is assumed to be fixed to constantly provide regulation capacity for the power system. The average ambient temperature and ventilation rate are assumed to be θ_o^{avg} and ν_i^{avg}. Then Eq. (18) can be derived as:

$$\begin{aligned} &C_i(\theta_i^{\mathrm{II}} - \theta_i^{\mathrm{I}}) = T_{\mathrm{D}}\gamma_i^{\mathrm{avg}}\theta_o^{\mathrm{avg}} - \int_{t_{\mathrm{I}}}^{t_{\mathrm{II}}} \gamma_i^{\mathrm{avg}}\theta_i(t)dt - T_{\mathrm{D}}\eta_i P^{\mathrm{reg}}_{\mathrm{HVAC},i}, \\ \Leftrightarrow\ & P^{\mathrm{reg}}_{\mathrm{HVAC},i} = \frac{\gamma_i^{\mathrm{avg}}\theta_o^{\mathrm{avg}}}{\eta_i} - \frac{C_i(\theta_i^{\mathrm{II}} - \theta_i^{\mathrm{I}})}{T_{\mathrm{D}}\eta_i} - \frac{\gamma_i^{\mathrm{avg}}}{T_{\mathrm{D}}\eta_i}\int_{t_{\mathrm{I}}}^{t_{\mathrm{II}}} \theta_i(t)dt, \\ &\forall i \in \mathcal{I}, \forall t \in \mathcal{T}. \end{aligned} \tag{19}$$

Eq. (19) indicates that if we want to obtain the inverter-based HVAC's adjustable operating power $P^{\mathrm{reg}}_{\mathrm{HVAC},i}$, the integral of the indoor temperature $\theta_i(t)$ from time t_{I} to t_{II} should be calculated. However, as shown in Fig. 4, the variation curve of

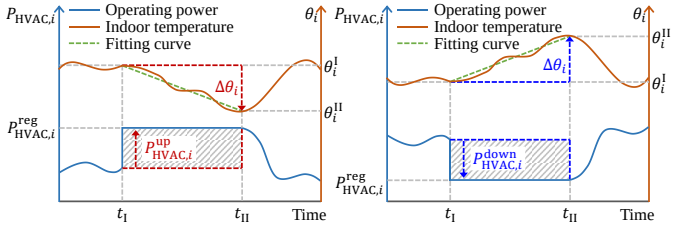

(a) Up-regulation. (b) Down-regulation.

Fig. 4. Inverter-based HVAC's regulation process in cooling state in summer.

the indoor temperature $\theta_i(t)$ is hard to be expressed as explicit formulae. To address this issue, we approximate the indoor temperature deviation as a monotonic linear function:

$$\theta_i(t) = \theta_i^{\mathrm{I}} + \frac{\theta_i^{\mathrm{II}} - \theta_i^{\mathrm{I}}}{t_{\mathrm{II}} - t_{\mathrm{I}}} t, \ \forall i \in \mathcal{I}, \forall t \in [t_{\mathrm{I}}, t_{\mathrm{II}}]. \tag{20}$$

Substituting Eq. (20) into Eq. (19) yields:

$$P^{\mathrm{reg}}_{\mathrm{HVAC},i} = \frac{\gamma_i^{\mathrm{avg}}\theta_o^{\mathrm{avg}}}{\eta_i} - \frac{C_i(\theta_i^{\mathrm{II}} - \theta_i^{\mathrm{I}})}{T_{\mathrm{D}}\eta_i} - \frac{\gamma_i^{\mathrm{avg}}(\theta_i^{\mathrm{II}} + \theta_i^{\mathrm{I}})}{2\eta_i}, \forall i \in \mathcal{I}. \tag{21}$$

In Eq. (21), parameters of the building, the inverter-based HVAC, and the ambient (e.g., C_i, γ_i^{avg}, η_i, θ_o^{avg}) depend on the physical quantities themselves, while not the users or the real-time LEM. The initial indoor temperature θ_i^{I} is a real-time measurement value. The users can only decide the remaining two quantities, the regulation duration time T_{D} and the desired indoor temperature after regulation θ_i^{II}. Therefore, Eq. (21) can be regarded as a function of two variables, i.e., $P^{\mathrm{reg}}_{\mathrm{HVAC},i}(T_{\mathrm{D}}, \theta_i^{\mathrm{II}})$. When the regulation duration time T_{D} is determined, we can get the relationship between the adjustable temperature θ_i^{II} and the adjustable power $P^{\mathrm{reg}}_{\mathrm{HVAC},i}$ in different inertia scenarios θ_i^{I}.

As shown in Fig. 5, the adjustable value of the inverter-based HVAC's operating power during the regulation process is calculated based on two scenarios, i.e., the regulation duration time T_{D} is set as 15min and 30min, respectively. The inverter-based HVAC is operating in a cooling state in summer, whose parameters are shown in detail in Appendix A. The diagonal elements of the matrix in Fig. 5 indicate that the indoor temperature maintains constant during the regulation process. With the decrease of the set indoor temperature, the inverter-based HVAC's operating power will be higher (e.g., it is 2.132kW in $\theta_i^{\mathrm{I}} = \theta_i^{\mathrm{II}} =$ 22ºC scenario and 1.427kW in $\theta_i^{\mathrm{I}} = \theta_i^{\mathrm{II}} =$ 26ºC scenario). Moreover, with the increase of the initial indoor temperature θ_i^{I}, the inverter-based HVAC has to operate with a larger power to reach the same target temperature θ_i^{II}. For example, in Fig. 5(a), the operating power is increased from 2.132kW in $\theta_i^{\mathrm{I}} = 22$ºC scenario to 2.602kW in $\theta_i^{\mathrm{I}} = 26$ºC scenario for reaching the same indoor temperature $\theta_i^{\mathrm{II}} = 22$ºC. Besides, by comparing Fig. 5(a) and Fig. 5(b), it can be seen that with the increase of the regulation duration time T_{D}, the left upper triangular matrix elements become larger and the right lower triangular matrix elements become smaller. Because the left upper triangular matrix elements mean the indoor temperature is increased from θ_i^{I} to θ_i^{II} after the regulation (i.e., the down-regulation scenario), in which longer duration time can decrease the power reduction value. By contrast, the right lower triangular matrix elements mean the indoor temperature is decreased from θ_i^{I} to θ_i^{II} after the regulation (i.e., the up-regulation scenario), in which a

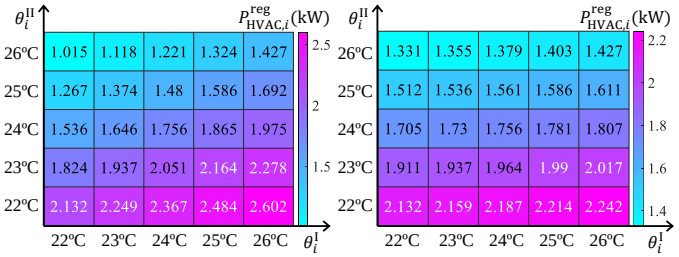

(a) Regulation duration time is 15min. (b) Regulation duration time is 30min.

Fig. 5. The adjustable value of the inverter-based HVAC's operating power in cooling state in summer.

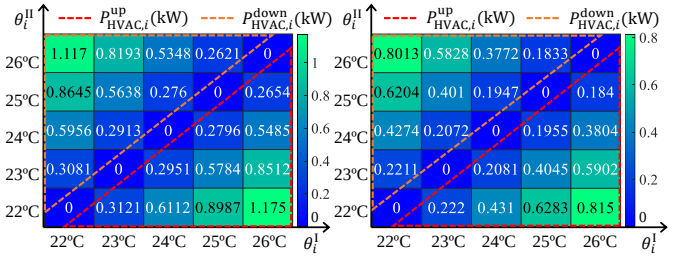

(a) Regulation duration time is 15min. (b) Regulation duration time is 30min.

Fig. 6. The up- and down- regulation capacties of the inverter-based HVAC in cooling state in summer with the comfortable constraints 22~26ºC.

longer duration time can decrease the power increment value. To sum up, a longer duration time can decrease both up-and down-regulation capacities of the inverter-based HVAC.

In the practical execution process, the minimum and maximum indoor temperature deviations are generally set by the user in advance (i.e., $\theta_i^{\min} \le \theta_i \le \theta_i^{\max}$). Then the maximum available up-and down-regulation capacities of the inverter-based HVAC can be calculated as:

$$\begin{cases} P_{\mathrm{HVAC},i}^{\mathrm{up,max}} = P_{\mathrm{HVAC},i}^{\mathrm{reg}}(T_{\mathrm{D}},\theta_i^{\min}) - P_{\mathrm{HVAC},i}(t_{\mathrm{I}}), & \forall i \in \mathcal{I}, \\ P_{\mathrm{HVAC},i}^{\mathrm{down,max}} = P_{\mathrm{HVAC},i}(t_{\mathrm{I}}) - P_{\mathrm{HVAC},i}^{\mathrm{reg}}(T_{\mathrm{D}},\theta_i^{\max}), & \forall i \in \mathcal{I}, \end{cases} \tag{22}$$

where $P_{\mathrm{HVAC},i}^{\mathrm{reg}}(T_{\mathrm{D}},\theta_i^{\min})$ and $P_{\mathrm{HVAC},i}^{\mathrm{reg}}(T_{\mathrm{D}},\theta_i^{\max})$ should be within the inverter-based HVAC's operating power range $[0, P_{\mathrm{HVAC},i}^{\mathrm{rate}}]$.

Based on the inverter-based HVAC's parameters in Fig. 5, its up-and down-regulation capacities in cooling state in summer can be calculated as Fig. 6 ($\theta_i^{\min} = 22$ºC, $\theta_i^{\max} = 26$ºC). The diagonal elements of the matrix indicate different initial indoor temperature θ_i^{I}. When the indoor temperature remains constant (i.e., $\theta_i^{\mathrm{II}} = \theta_i^{\mathrm{I}}$), the inverter-based HVAC does not provide up- or down-regulation capacities (i.e., zero elements). When the indoor temperature decreases (i.e., $\theta_i^{\mathrm{II}} < \theta_i^{\mathrm{I}}$), the inverter-based HVAC can provide up-regulation capacity (i.e., lower triangular matrix elements). When the indoor temperature increases (i.e., $\theta_i^{\mathrm{II}} > \theta_i^{\mathrm{I}}$), the inverter-based HVAC can provide down-regulation capacity (i.e., upper triangular elements).

C. *Multi-level Bidding Strategy of Inverter-based HVAC*

The evaluated up-and down-regulation capacities in Eq. (22) are the maximum allowable adjustable values, which cannot be utilized directly to bid in the LEM. Because the bidding quantities should be submitted with corresponding prices in block forms, as shown in Fig. 7. The horizontal coordinate is the bidding quantity of the *i*-th inverter-based HVAC's power consumption, and the vertical coordinate is its bidding price. The objective of the multi-level bidding strategy is to decrease the electricity cost and maintain the indoor temperature always

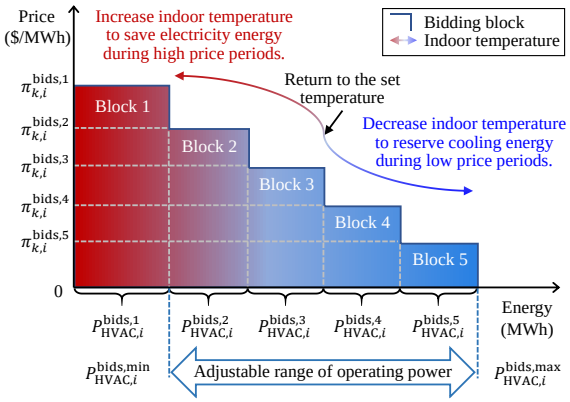

Fig. 7. The dynamic multi-level bidding strategy of the inverter-based HVAC in the real-time LEM.

within the user's constraints. Then the bidding blocks in Fig. 7 can be divided into three conditions: i) When the D-LMP is within the normal range, the indoor temperature is regulated to be equal to the set value (i.e., the most desired indoor temperature). ii) When the D-LMP is at a high level, the inverter-based HVAC's power consumption will be decreased to reduce the electricity cost. This process can cause a slight increase in the indoor temperature, while it is still within the allowable adjustment range. iii) When the D-LMP is at a low level, the inverter-based HVAC's power consumption will be increased to decrease the indoor temperature within the allowable adjustment range. In this manner, the building can reserve some cooling capacities to obtain more down-regulation capacity to decrease the electricity cost during high D-LMP periods. Based on these three conditions, the multi-level bidding quantities of inverter-based HVACs are designed as five blocks:

$$\begin{cases} P_{\mathrm{HVAC},i}^{\mathrm{bids},1}(t) = P_{\mathrm{HVAC},i}^{\mathrm{bids,min}} = P_{\mathrm{HVAC},i}^{\mathrm{reg}}(T_{\mathrm{D}},\theta_i^{\max}), \\ P_{\mathrm{HVAC},i}^{\mathrm{bids},2}(t) = P_{\mathrm{HVAC},i}^{\mathrm{bids},3}(t) \\ \qquad = (P_{\mathrm{HVAC},i}^{\mathrm{reg}}(T_{\mathrm{D}},\theta_i^{\mathrm{set}}) - P_{\mathrm{HVAC},i}^{\mathrm{reg}}(T_{\mathrm{D}},\theta_i^{\max}))/2, \\ P_{\mathrm{HVAC},i}^{\mathrm{bids},4}(t) = P_{\mathrm{HVAC},i}^{\mathrm{bids},5}(t) \\ \qquad = (P_{\mathrm{HVAC},i}^{\mathrm{reg}}(T_{\mathrm{D}},\theta_i^{\min}) - P_{\mathrm{HVAC},i}^{\mathrm{reg}}(T_{\mathrm{D}},\theta_i^{\mathrm{set}}))/2, \\ \forall i \in \mathcal{I}, \forall t \in \mathcal{T}. \end{cases} \tag{23}$$

where blocks 1 and 5 are the minimum and maximum operating power, respectively, for maintaining the comfortable indoor temperature requirement. Block 3 is $P_{\mathrm{HVAC},i}^{\mathrm{reg}}(T_{\mathrm{D}},\theta_i^{\mathrm{set}})$ to recover the indoor temperature to the set value. The remaining two blocks 2 and 4 are for adjusting the indoor temperature to the middle states, to save cost and reserve energy, respectively.

Apart from the bidding quantities in Eq. (23), the corresponding bidding price strategies should also be designed. First of all, to guarantee the basic (i.e., the minimum) operating power of the inverter-based HVAC in block 1, the bidding price in the first block is set to be equal to the cap value:

$$\pi_{k,i}^{\mathrm{bids},1}(t) = \pi_k^{\mathrm{cap}}, \quad \forall i \in \mathcal{I}, \forall k \in \mathcal{N}_{\mathrm{bus}}, \forall t \in \mathcal{T}. \tag{24}$$

where π_k^{cap} is the price cap at the *k*-th bus (i.e., the permissible maximum bidding price in the real-time LEM); $\pi_{k,i}^{\mathrm{bids},1}$ is the *i*-th HVAC's first block bidding price at the *k*-th bus.

The proposed bidding price strategy refers to the historical D-LMPs in previous hours T_p, which can be equal to 4, 16, 48, and 96 when previous periods of 1 hour, 4 hours, 12 hours, and

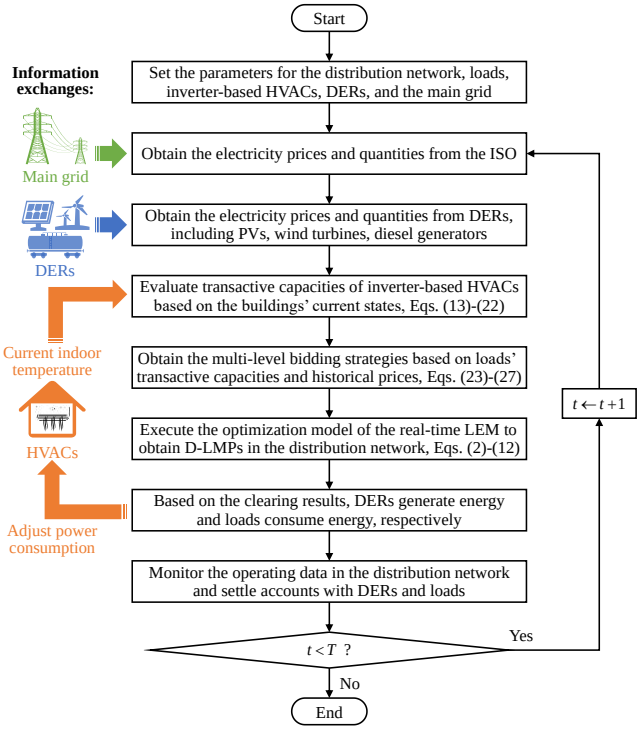

Fig. 8. The implementation procedure of the LEM for distribution network.

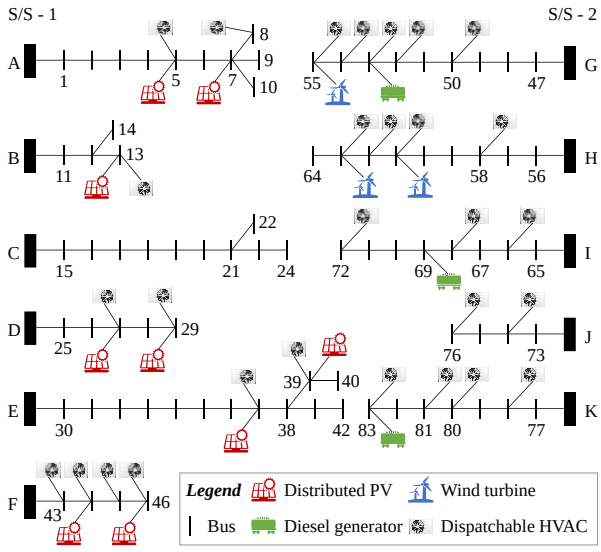

Fig. 9. The 84-bus distribution network with distributed PVs on 9 buses, wind turbines on 3 buses, diesel generators on 3 buses, and dispatchable inverter-based HVACs on 29 buses.

24 hours are considered. Specifically, the bidding price strategy refers to the minimum D-LMP $\pi_{k,T_p}^{\min}(t)$ and the average D-LMP $\pi_{k,T_p}^{\text{avg}}(t)$ in previous periods T_p, which are calculated as:

$$\begin{cases} \pi_{k,T_p}^{\min}(t) = \min[\pi_k(t-1),\cdots,\pi_k(t-T_p)], \\ \pi_{k,T_p}^{\text{avg}}(t) = \dfrac{1}{T_p}\displaystyle\sum_{\tau=t-T_p}^{t-1}\pi_k(\tau),\ \forall k \in \mathcal{N}_{\text{bus}}, \forall (t,\tau) \in \mathcal{T}. \end{cases} \tag{25}$$

Then the bidding prices of blocks 2~5 can be designed based on the D-LMP's changing trend. During the D-LMP's rising trend (i.e., $\pi_k(t-1) \geq \pi_{k,T_p}^{\text{avg}}(t)$), the bidding prices are set as follows:

$$\begin{cases} \pi_{k,i}^{\text{bids},2}(t) = \pi_k(t-1),\ \pi_{k,i}^{\text{bids},3}(t) = \pi_{k,T_p}^{\text{avg}}(t), \\ \pi_{k,i}^{\text{bids},4}(t) = (\pi_{k,T_p}^{\text{avg}}(t) + \pi_{k,T_p}^{\min}(t))/2, \\ \pi_{k,i}^{\text{bids},5}(t) = \pi_{k,T_p}^{\min}(t), \forall i \in \mathcal{I}, \forall k \in \mathcal{N}_{\text{bus}}, \forall t \in \mathcal{T}. \end{cases} \tag{26}$$

By contrast, during the D-LMP's downward trend (i.e., $\pi_k(t-1) < \pi_{k,T_p}^{\text{avg}}(t)$), the bidding prices are set as follows:

$$\begin{cases} \pi_{k,i}^{\text{bids},2}(t) = \pi_{k,T_p}^{\text{avg}}(t),\ \pi_{k,i}^{\text{bids},3}(t) = \pi_k(t-1), \\ \pi_{k,i}^{\text{bids},4}(t) = (\pi_k(t-1) + \alpha\pi_{k,T_p}^{\min}(t))/2, \\ \pi_{k,i}^{\text{bids},5}(t) = \alpha\pi_{k,T_p}^{\min}(t), \forall i \in \mathcal{I}, \forall k \in \mathcal{N}_{\text{bus}}, \forall t \in \mathcal{T}, \end{cases} \tag{27}$$

where $\alpha \in [0,1]$ is the adjustment factor for decreasing the bidding price of block 5. In this manner, the inverter-based HVAC can reserve more up-regulation capacity to utilize cheaper electricity prices during the D-LMP's downward trend.

Each inverter-based HVAC's multi-level bidding strategy in Eqs. (23)-(27) will be regulated dynamically in real-time according to its operating state, the current indoor temperature, the user's desired temperature, the regulation duration time, the local ambient temperature, and the latest historical D-LMPs. In this manner, all the inverter-based HVACs' bidding strategies are customized and flexibly regulated based on their operating states and the price clearing results in the real-time LEM, to decrease the user's electricity cost and maintain their comfortable indoor temperature requirements all the time.

The implementation procedure of the real-time LEM for the distribution network is shown in Fig. 8. The first step is to set the parameters for the distribution network, loads, inverter-based HVACs, DERs, and the main grid. Then, the DSO obtains the electricity prices and quantities from the ISO in the second step and DERs in the third step, respectively. Next, according to Eqs. (13)-(22), the transactive capacities of inverter-based HVACs are evaluated based on the buildings' current states. According to Eqs. (23)-(27), the multi-level bidding strategy is obtained based on loads' transactive capacities and historical prices. According to Eqs. (2)-(12), the DSO executes the optimization model of the real-time LEM to obtain D-LMPs in the distribution network. Based on the clearing results, DERs generate energy and loads consume energy, respectively. Finally, the operating data in the distributed network are monitored for the settlement of DERs and loads. If another market session will be executed (i.e., $t < T$), steps 2-8 will be carried out again.

There are mainly four information exchange processes: i) The main grid (i.e., the ISO) provides the electricity prices and energy quantities to the distribution network (i.e., the DSO) with the communication time of around 50ms [56]; ii) DERs (including PVs, wind turbines, and diesel generators) offer the output energy quantities and prices to the DSO with the communication time of around 50ms [57]; iii) The transactive controllers of HVACs obtain the current indoor temperatures with the communication time of around 10ms [28]. On this basis, the transactive controllers can evaluate the available regulation capacities for providing bidding capacities and prices to the DSO; iv) HVACs adjust their power consumptions, which can change the indoor temperatures to further impact the next time-slot's available regulation capacities.

The models and methods are formulated in MATLAB R2019b on a computer with Intel (R) Core (TM) i7-9700 CPU,

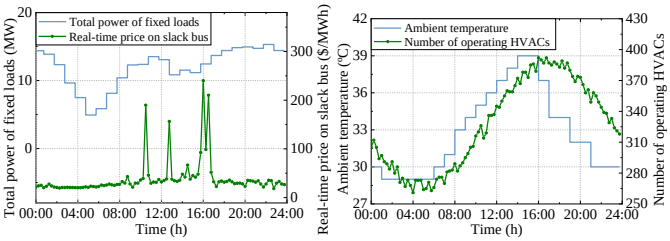

(a) The total power of fixed loads and real-time price on slack bus.

(b) The dynamic operating number of HVACs and ambient temperature.

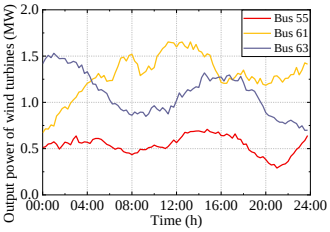

(c) The fluctuating output power of wind turbines.

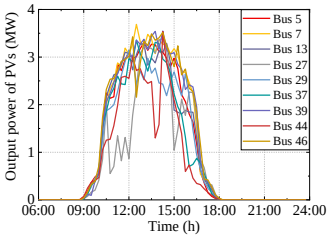

(d) The fluctuating output power of PVs.

Fig. 10. The initial parameters of the 84-bus distribution network.

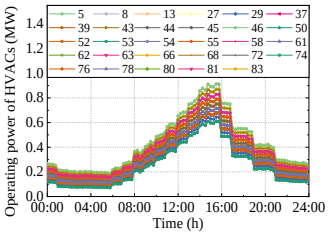

(a) The operating power of inverter-based HVACs on 29 buses in Case 1.

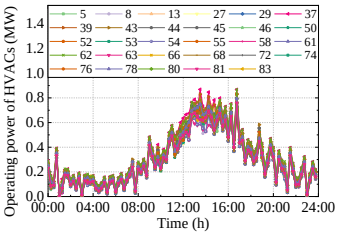

(b) The operating power of inverter-based HVACs on 29 buses in Case 2.

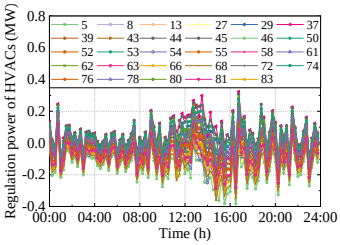

(c) The regulation power of inverter-based HVACs in the real-time LEM.

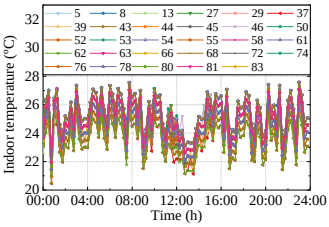

(d) The dynamic indoor temperature during HVACs' regulation process.

Fig. 11. The results of dispatchable inverter-based HVACs in real-time LEM.

clocking at 3.00 GHz and 16.0 GB RAM. The execution time for clearing the market is 0.3241s for each dispatch time slot. The total execution time is 0.4341s, which is enough for the real-time LEM because the informatics process and calculation are carried out in the pre-operating slot (i.e, 15min earlier).

IV. Numerical Studies

A. Test System

The proposed models and methods are tested based on a realistic 84-bus distribution network of Taiwan Power Company, as shown in Fig. 9 [58], [59]. The distribution network is a radial topology and connects with the main grid through one slack bus (i.e., all the letters A ~ K in Fig. 9 indicate the slack bus). Numbers 1~ 83 indicate the distribution network's buses. All the buses have fixed loads, whose power consumption changes with time while cannot be regulated, as shown in Fig. 10(a). The voltage limitation of the distribution network is $\pm 10\%$ of its nominal value. The current limitations of feeders are between 60~275A. Besides, letters A~M in Fig. 9 indicate the slack bus, which is connected with the main grid through two 20MVA, 33/11.4kV transformers. The real-time electricity price of the main grid adopts the realistic data in PJM market in the US, as shown in Fig. 10(a).

Dispatchable inverter-based HVACs are distributed on 29 buses, as shown in Fig. 9. Each bus has 400 inverter-based HVACs, whose operating number is dynamic during a day depending on the users at home and the ambient temperature, as shown in Fig. 10(b). The indoor temperature is set randomly by the users between 23ºC and 25ºC. The maximum allowable indoor temperature deviation is ± 2ºC. It is assumed that each inverter-based HVAC is equipped with a transactive controller, which is authorized by its user to make decisions and participate in the real-time LEM. The transactive capacity evaluation method and multi-level bidding strategy in Eqs. (21)-(27) have been built-in to the transactive controller. Other parameters of inverter-based HVACs and buildings' thermal characteristics are shown in detail in Appendix A.

The DERs in the distribution network include PVs on 9 buses, wind turbines on 3 buses, and diesel generators on 3 buses, as shown in Fig. 9. The wind turbines' and PVs' output power are based on the realistic tested data in China, as shown in Fig. 10(c) and Fig. 10(d), respectively. The diesel generators on buses 53, 69, and 83 have the same capacity of 0.66MW. Each bus has 4 diesel generators to offer constant quantity with constant prices as follows: 0.66MW@100$/MWh, 0.66MW@150$/MWh, 0.66MW@200$/MWh, 0.66MW@300$/MWh. The time slot of the real-time LEM is 15min.

Two cases are analyzed in this subsection. **Case 1:** Inverter-based HVACs do not participate in the real-time LEM; **Case 2:** the operating inverter-based HVACs in the distribution network participate in the real-time LEM with $T_p = 4$.

B. Results Analysis of Dispatchable Inverter-based HVACs

As shown in Fig. 11(a), the operating power of inverter-based HVACs on 29 buses fluctuates with time in Case 1, all of which reach peak values at around 14:00~16:00. The first reason is that the ambient temperature is the highest at that time. The second reason is that the number of inverter-based HVACs in the ON-state is large during that period, as shown in Fig. 10(b). By contrast, Fig. 11(b) shows the operating power of inverter-based HVACs on 29 buses in Case 2, which has more fluctuations compared with the load curves in Fig. 11(a). This is because the inverter-based HVACs' operating power is not only impacted by the ambient temperature and ON-state's number but it is also regulated based on the bidding results in the real-time LEM. In other words, the proposed real-time LEM motivates some "free" regulation capacities in the distribution network from transactive inverter-based HVACs since they react to D-LMPs.

The transactive capacities are shown in Fig. 11(c), where positive values indicate increasing the inverter-based HVACs' operating power to reserve cooling capacities in buildings during low D-LMP periods. By contrast, the negative values mean decreasing the inverter-based HVACs' operating power to save energy cost during high D-LMP periods. This regulation

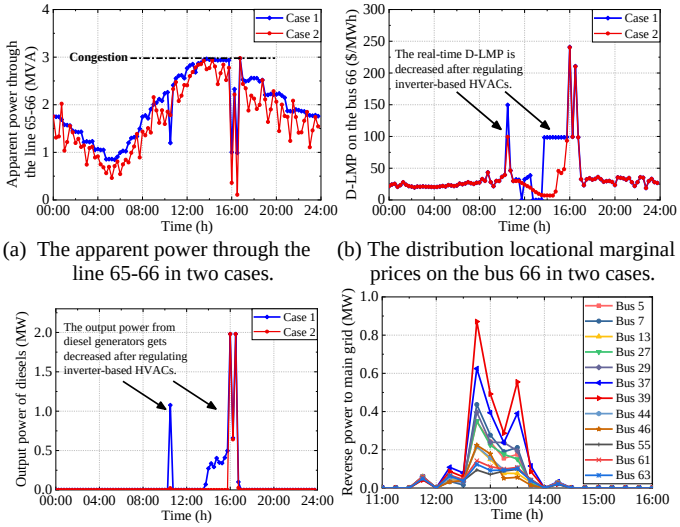

(a) The apparent power through the line 65-66 in two cases.

(b) The distribution locational marginal prices on the bus 66 in two cases.

(c) Output power of diesel generators on the bus 69 in two cases.

(d) The export power of local renewable energies to the main grid.

Fig. 12. Impact analysis on the distribution network of inverter-based HVACs.

TABLE I
ELECTRICITY COST-SAVING UNDER DIFFERENT PARTICIPATION RATES

Participation Rates of HVACs	0%	25%	50%	100%
Total cost of inverter-based HVACs ($)	10,367	8,488	7,969	7,568
Cost-saving of inverter-based HVACs	N/A	18.12%	23.13%	27.00%
Total cost of all the loads ($)	20,794	18,290	17,612	17,254
Cost-saving of all the loads	N/A	12.04%	15.30%	17.02%
Reverse energy of renewables (MWh)	3.34	2.59	2.21	0
Output energy of diesels (MWh)	5.13	4.01	3.88	3.63

process also has influences on the indoor temperature. As shown in Fig. 11(d), the indoor temperatures will not always be equal to the set-point values, while they fluctuate within their allowable deviation ranges ± 2ºC. This comfort constraint verifies the effectiveness of the proposed transactive capacity evaluation method on inverter-based HVACs.

C. *Impact Analysis on the Distribution Network*

Transactive inverter-based HVACs in the real-time LEM have many impacts on the operation of the distribution network. First of all, the network congestions are reduced evidently, as shown in Fig. 12(a). The maximum apparent power through line 65-66 is 2.97MVA. Congestion occurs on this line at 10 time slots (i.e., 13:45-15:45 and 16:45) in Case 1, due to the large operating power of loads. After the regulation of HVACs' operating power in Case 2, the congestion occurrence is significantly reduced to only 1 time slot (i.e., 16:45). The relief of line congestion is also reflected in the D-LMP at bus 66 and in the operation state of diesel generators on bus 69, as shown in Figs. 12(b) and (c), respectively. During the congestion time slots in Case 1, the diesel generators on bus 69 provide power to the loads on bus 66, which improves its D-LMP in the time 13:45-15:45. Table I shows that the total output energy of diesel generators decreases from 5.13MWh to 3.63MWh when inverter-based HVACs participate in the real-time LEM. Besides, another peak power generation period of diesel generators occurs at 16:00-16:30 in Fig. 12(c), because the real-time electricity price of the main grid is very high at this period and exceeds the bidding price of diesel generators. It results in the increased utilization of local diesel generators.

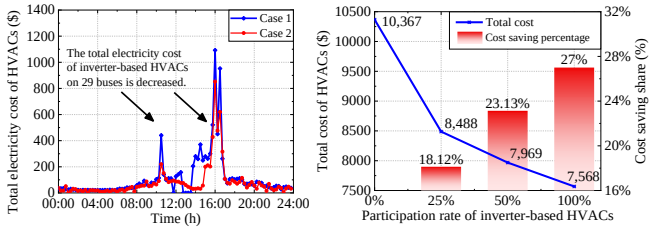

(a) Cost of inverter-based HVACs.

(b) Participation rate impacts on the cost.

Fig. 13. The cost of inverter-based HVACs in the real-time LEM.

TABLE II
ELECTRICITY COST-SAVING UNDER DIFFERENT BIDDING STRATEGIES

Historical time horizons of T_p	4 (1h)	16 (4h)	48 (12h)	96 (24h)
Total cost of inverter-based HVACs ($)	7,568	7,398	7,514	7,423
Cost-saving of inverter-based HVACs	27.00%	28.64%	27.52%	28.40%
Total cost of all the loads ($)	17,254	17,051	17,214	17,081
Cost-saving of all the loads	17.02%	18.00%	17.22%	17.86%
Reverse energy of renewables (MWh)	0	0	0	0
Output energy of diesels (MWh)	3.63	3.62	3.62	3.65

Furthermore, transactive inverter-based HVACs make more distributed renewable energies be utilized locally. As shown in Fig. 12(d), around 3.34MWh output energy from PVs and wind turbines have to be exported to the main grid in Case 1, because the output power of local renewable energies exceeds loads' consumed power in some time slots. However, when inverter-based HVACs participate in the real-time LEM in Case 2, the exported energy becomes zero. This is because renewable energies' bidding price is assumed to be zero, and inverter-based HVACs will vary their power consumption proportionally to the output power of renewable energies to reduce the cost.

D. *Discussions and Comparisons of Different Participation Rates and Bidding Strategies*

Table I shows the electricity cost-saving results under different participation rates of inverter-based HVACs. It can be seen that the total cost of inverter-based HVACs continuously decreases with the increase of participation rate. For example, it decreases from 10,367$ in the 0% scenario to 7,568$ in the 100% scenario, which falls by around 27%. As shown in Fig. 13(a), the cost of inverter-based HVACs reduces most of the time during the day. Furthermore, the transactive energy framework for inverter-based HVACs also contributes to the decrease of the total cost of all the loads. It can be seen from Table I that the total cost decreases from 20,794$ in the 0% scenario to 17,254$ in the 100% scenario. The total cost falls by around 17.02% because the interactive regulation of inverter-based HVACs reduces the D-LMPs, which are also the settlement prices of conventional unchangeable loads. In addition, the exported energy of distributed renewable energies to the main grid continuously decreases from 3.34MWh to 0MWh, because inverter-based HVACs vary their power consumption to consume more fluctuating renewable energies for reducing the energy cost. The output energy of diesel generators also correspondingly decreases from 5.13MWh to 3.63MWh, because more energy is from the distributed renewable energies in the 100% scenario.

The impacts of time horizons are analyzed by comparing four bidding strategies, i.e., considering different horizons of

historical D-LMPs $T_p = 4$, 16, 48, and 96. The results are shown in Table II. It can be seen that the reverse energy of renewables is all zero in the four bidding strategies. The total cost of all the loads is among 17,051-17,254$. The output energy of diesel generators is among 3.62-3.65MWh. The best cost-saving scenario is $T_p = 16$, which can reach 28.64% and 18.00% for the inverter-based HVACs and all the loads, respectively. Nevertheless, different bidding strategies obtain similar results in general, because HVACs' cooling capacities are stored only by the buildings' thermal inertia and cannot be reserved for a long time. Hence the bidding strategies with longer time horizons do not have significant impacts on the schedule of HVACs.

V. Conclusion

This paper proposes a real-time LEM and a DSO's optimization framework considering multiple participants, including rapidly increasing inverter-based HVACs, PVs, and wind turbines. A transactive capacity evaluation method is proposed for inverter-based HVACs to participate in the real-time LEM, which considers the regulation duration time, the dynamic ambient temperature, the building's heat conduction, the air ventilation, and the user's comfort requirements. Based on the available transactive capacities and the historical D-LMPs, a multi-level bidding strategy is developed for inverter-based HVACs. Numerical studies verify that the users' cost can be decreased by 27% under guaranteeing their comfort requirements. More fluctuating output energy of wind turbines and PVs can be utilized locally, which improves the system's efficiency and alleviate the distribution network's congestions.

In the future, we would like to pay attention to the increasing ice storage air conditionings (ISACs), because they are better regulation resources to avoid the impact on users' comforts during the regulation process. ISACs are generally used for large district cooling systems [60] and can storage cooling capacity for a long time (e.g., one day or longer time). The day-ahead market and optimization methods can be developed for ISACs.

Appendix A

The inverter-based HVACs' parameters and corresponding buildings' thermal parameters are based on Chinese National Standards and realistic tested data in China. Each inverter-based HVACs' rated power distributes among 1.5~3.0 kW; the energy efficiency ratio η_i is distributed among 2.2~3.2; the regulation ranges of compressors' rotating frequency f_i are 20~100Hz; the coefficients ξ_i and σ_i are 0.01~0.03 kW/Hz and 0.005~0.01 kW, respectively. The bidding price's adjustment factor α is 0.8. The corresponding building's thermal capacity C_i ranges among 100~300 kJ/ºC; the thermal resistance R_i ranges among 0.15~0.75 ºC/kW; the ventilation rate ν_i changes among 0.5~2 h^{-1}.

References

[1] *Renewables 2020 Global Status Report*, REN21, 2020. [Online]. Available: https://www.ren21.net/reports/global-status-report.

[2] F. Luo, G. Ranzi, C. Wan, Z. Xu and Z. Y. Dong, "A multistage home energy management system with residential photovoltaic penetration," *IEEE Trans. Ind. Informat.*, vol. 15, no. 1, pp. 116-126, Jan. 2019.

[3] D. Zhang, H. Zhu, H. Zhang, H. H. Goh, H. Liu and T. Wu, "Multi objective optimization for smart integrated energy system considering demand responses and dynamic prices," *IEEE Trans. Smart Grid*, early access.

[4] E. Rezaei and H. Dagdougui, "Optimal real-time energy management in apartment building integrating microgrid with multizone HVAC control," *IEEE Trans. Ind. Informat.*, vol. 16, no. 11, pp. 6848-6856, Nov. 2020.

[5] Q. Shi, C. Chen, A. Mammoli and F. Li, "Estimating the profile of incentive-based demand response (IBDR) by integrating technical models and social-behavioral factors," *IEEE Trans. Smart Grid*, vol. 11, no. 1, pp. 171-183, Jan. 2020.

[6] M. Ghorbanian, S. H. Dolatabadi, P. Siano, I. Kouveliotis-Lysikatos and N. D. Hatziargyriou, "Methods for flexible management of blockchain-based cryptocurrencies in electricity markets and smart grids," *IEEE Trans. Smart Grid*, vol. 11, no. 5, pp. 4227-35, Apr. 2020.

[7] F. Lezama, J. Soares, P. Hernandez-Leal, M. Kaisers, T. Pinto and Z. Vale, "Local energy markets: paving the path toward fully transactive energy systems," *IEEE Trans. Power Syst.*, vol. 34, no. 5, pp. 4081-8, Sep. 2019.

[8] M. Daneshvar, B. Mohammadi-Ivatloo, K. Zare and S. Asadi, "Two-stage robust stochastic model scheduling for transactive energy based renewable microgrids," *IEEE Trans. Ind. Informat.*, vol. 16, no. 11, pp. 6857-6867, Nov. 2020.

[9] M. Daneshvar, B. Mohammadi-Ivatloo, K. Zare, S. Asadi and A. Anvari-Moghaddam, "A novel operational model for interconnected microgrids participation in transactive energy market: a hybrid IGDT approach," *IEEE Trans. Ind. Informat.*, vol. 17, no. 6, pp. 4025-35, Jun. 2021.

[10] H. S. V. S. K. Nunna and D. Srinivasan, "Multiagent-based transactive energy framework for distribution systems with smart microgrids," *IEEE Trans. Ind. Informat.*, vol. 13, no. 5, pp. 2241-2250, Oct. 2017.

[11] M. S. H. Nizami, M. J. Hossain and E. Fernandez, "Multiagent-based transactive energy management systems for residential buildings with distributed energy resources," *IEEE Trans. Ind. Informat.*, vol. 16, no. 3, pp. 1836-1847, Mar. 2020.

[12] J. Lin, M. Pipattanasomporn and S. Rahman, "Comparative analysis of auction mechanisms and bidding strategies for P2P solar transactive energy markets," *Appl. energy*, vol. 255, p. 113687, Dec. 2019.

[13] M. Rayati and A. M. Ranjbar, "Resilient transactive control for systems with high wind penetration based on cloud computing," *IEEE Trans. Ind. Informat.*, vol. 14, no. 3, pp. 1286-1296, Mar. 2018.

[14] J. Hu, G. Yang, C. Ziras and K. Kok, "Aggregator operation in the balancing market through network-constrained transactive energy," *IEEE Trans. on Power Syst.*, vol. 34, no. 5, pp. 4071-4080, Sep. 2019.

[15] Z. Yang, J. Hu, X. Ai, J. Wu and G. Yang, "Transactive energy supported economic operation for multi-energy complementary microgrids," *IEEE Trans. Smart Grid*, vol. 12, no. 1, pp. 4-17, Jan. 2021.

[16] J. Li, C. Zhang, Z. Xu, J. Wang, J. Zhao and Y. -J. A. Zhang, "Distributed transactive energy trading framework in distribution networks," *IEEE Trans. Power Systems*, vol. 33, no. 6, pp. 7215-7227, Nov. 2018.

[17] Y. Wang, Z. Huang, M. Shahidehpour, L. L. Lai, Z. Wang and Q. Zhu, "Reconfigurable distribution network for managing transactive energy in a multi-microgrid system," *IEEE Trans. Smart Grid*, vol. 11, no. 2, pp. 1286-1295, Mar. 2020.

[18] Karimi H, Bahmani R, Jadid S, Makui A, "Dynamic transactive energy in multi-microgrid systems considering independence performance index: A multi-objective optimization framework," *Int. J. Electr. Power Energy Syst.*, vol. 126, p. 106563, Mar. 2021.

[19] Z. Liu, L. Wang and L. Ma, "A transactive energy framework for coordinated energy man-agement of networked microgrids with distributionally robust optimization," *IEEE Trans. Power Syst.*, vol. 35, no. 1, pp. 395-404, Jan. 2020.

[20] W. Liu, J. Zhan and C. Y. Chung, "A novel transactive energy control mechanism for collaborative networked microgrids," *IEEE Trans. Power Syst.*, vol. 34, no. 3, pp. 2048-2060, May 2019.

[21] Q. Yang and H. Wang, "Blockchain-empowered socially optimal transactive energy system: framework and implementation," *IEEE Trans. Ind. Informat.*, vol. 17, no. 5, pp. 3122-3132, May 2021.

[22] Y. Xiao, X. Wang, P. Pinson and X. Wang, "Transactive energy based aggregation of prosumers as a retailer," *IEEE Trans. Smart Grid*, vol. 11, no. 4, pp. 3302-3312, Jul. 2020.

[23] M. Yan, M. Shahidehpour, A. Paaso, L. Zhang, A. Alabdulwahab and A. Abusorrah, "Distribution network-constrained optimization of peer-to-peer transactive energy trading among multi-microgrids," *IEEE Trans. Smart Grid*, vol. 12, no. 2, pp. 1033-1047, Mar. 2021.

[24] W. Gan, M. Yan, W. Yao and J. Wen, "Peer to peer transactive energy for multiple energy hub with the penetration of high-level renewable energy," *Appl. Energy*, vol. 295, p. 117027, Aug. 2021.

[25] K. Jhala, B. Natarajan, A. Pahwa and H. Wu, "Stability of transactive energy market-based power distribution system under data integrity attack," *IEEE Trans. Ind. Informat.*, vol. 15, no. 10, pp. 5541-5550, Oct. 2019.

[26] Y. Chen, D. Qi, H. Dong, C. Li, Z. Li and J. Zhang, "A FDI attack-resilient distributed secondary control strategy for islanded microgrids," *IEEE Trans. Smart Grid*, vol. 12, no. 3, pp. 1929-1938, May 2021.

[27] C. Feng, F. Wen, S. You, Z. Li, F. Shahnia and M. Shahidehpour, "Coalitional game-based transactive energy management in local energy communities," *IEEE Trans. Power Syst.*, vol. 35, no. 3, pp. 1729-1740, May 2020.

[28] H. Hui, Y. Ding, Q. Shi, F. Li, Y. Song and J. Yan, "5G network-based Internet of Things for demand response in smart grid: A survey on application potential," *Appl. Energy*, vol. 257, p. 113972, Jan. 2020.

[29] H. Zhu, H. H. Goh, D. Zhang, T. Ahmad, H. Liu, S. Wang, S. Li, T. Liu, H. Dai and T. Wu, "Key technologies for smart energy systems: Recent developments, challenges, and research opportunities in the context of carbon neutrality," *J. Clean. Prod.*, vol. 331, p. 129809, Nov. 2021.

[30] M. Alhaider and L. Fan, "Planning energy storage and photovoltaic panels for demand response with heating ventilation and air conditioning systems," *IEEE Trans. Ind. Informat.*, vol. 14, no. 11, pp. 5029-37, Nov. 2018.

[31] Y. Kim, "Optimal price based demand response of HVAC systems in multizone office buildings considering thermal preferences of individual occupants buildings," *IEEE Trans. Ind. Informat.*, vol. 14, no. 11, pp. 5060-5073, Nov. 2018.

[32] Z. Liu, Q. Wu, K. Ma, M. Shahidehpour, Y. Xue and S. Huang, "Two-stage optimal scheduling of electric vehicle charging based on transactive control," *IEEE Trans. Smart Grid*, vol. 10, no. 3, pp. 2948-58, Mar. 2018.

[33] M. Song, W. Sun, Y. Wang, M. Shahidehpour, Z. Li and C. Gao, "Hierarchical scheduling of aggregated TCL flexibility for transactive energy in power systems," *IEEE Trans. on Smart Grid*, vol. 11, no. 3, pp. 2452-2463, Nov. 2019.

[34] H. Hui, Y. Ding and M. Zheng, "Equivalent modeling of inverter air conditioners for providing frequency regulation service," *IEEE Trans. Ind. Electr.*, vol. 66, no. 2, pp. 1413-23, Apr. 2018.

[35] T. Chen, Q. Cui, C. Gao, Q. Hu, K. Lai, J. Yang, R. Lyu, H. Zhang and J. Zhang, "Optimal demand response strategy of commercial building-based virtual power plant using reinforcement learning," *IET Gener. Transm. Distrib.*, Apr. 2021.

[36] K. Ma, Y. Yu, B. Yang and J. Yang, "Demand-side energy management considering price oscillations for residential building heating and ventilation systems," *IEEE Trans. Ind. Informat.*, vol. 15, no. 8, pp. 4742-4752, Aug. 2019.

[37] B. Liu, M. Akcakaya and T. E. Mcdermott, "Automated control of transactive hvacs in energy distribution systems," *IEEE Trans. Smart Grid*, vol. 12, no. 3, pp. 2462-2471, May 2021.

[38] N. Mohammad and A. Rahman, "Transactive control of industrial heating–ventilation–air-conditioning units in cold-storage warehouses for demand response," *Sustain. Energy, Grids and Networks*, vol. 18, p. 100201, Jun. 2019.

[39] S. Behboodi, D. P. Chassin, N. Djilali and C. Crawford, "Transactive control of fast-acting demand response based on thermostatic loads in real-time retail electricity markets," *Appl. Energy*, vol. 210, p. 1310-20, Jan. 2018.

[40] F. Shen, Q. Wu, S. Huang, X. Chen, H. Liu and Y. Xu, "Two-tier demand response with flexible demand swap and transactive control for real-time congestion management in distribution networks," *Int. J. Electr. Power Energy Syst.*, vol. 114, p. 105399, Jan. 2020.

[41] T. Pinto, R. Faia, M. A. F. Ghazvini, J. Soares, J. M. Corchado and Z. Vale, "Decision support for small players negotiations under a transactive energy framework," *IEEE Trans. Power Syst.*, vol. 34, no. 5, pp. 4015-4023, Sep. 2019.

[42] S. Behboodi, D. P. Chassin, N. Djilali and C. Crawford, "Transactive control of fast-acting demand response based on thermostatic loads in real-time retail electricity markets," *Appl. Energy*, vol. 210, pp. 1310-1320, Jan. 2018.

[43] N. Lu, "An evaluation of the HVAC load potential for providing load balancing service", *IEEE Trans. Smart Grid*, vol. 3, no. 3, pp. 1263-1270, Sep. 2012.

[44] X. Zhang, M. Pipattanasomporn, T. Chen and S. Rahman, "An IoT-based thermal model learning framework for smart buildings," *IEEE Internet Things J.*, vol. 7, no. 1, pp. 518-527, Jan. 2020.

[45] *Analysis on Inverter Air Conditioners in China*, Information Network of Chinese Business, Technical Report, 2015.

[46] M. Song, C. Gao, H. Yan and J. Yang, "Thermal battery modeling of inverter air conditioning for demand response," *IEEE Trans. Smart Grid*, vol. 9, no. 6, pp. 5522-34, Mar. 2017.

[47] C. Zhang, Y. Xu, Z. Li and Z. Dong, "Robustly coordinated operation of a multi-energy microgrid with flexible electric and thermal loads," *IEEE Trans. Smart Grid*, vol. 10, no. 3, pp. 2765-75, Feb. 2018.

[48] S. Behboodi, D. P. Chassin, N. Djilali and C. Crawford, "Transactive control of fast-acting demand response based on thermostatic loads in real-time retail electricity markets," *Appl. Energy*, vol. 210, pp. 1310-20, Jan. 2018.

[49] Q. Shi, C. Chen, A. Mammoli and F. Li, "Estimating the profile of incentive-based demand response (IBDR) by integrating technical models and social-behavioral factors," *IEEE Trans. Smart Grid*, vol. 11, no. 1, pp. 171-183, Jan. 2020.

[50] K. Jhala, B. Natarajan, A. Pahwa and H. Wu, "Stability of transactive energy market-based power distribution system under data integrity attack," *IEEE Trans. Ind. Informat.*, vol. 15, no. 10, pp. 5541-5550, Oct. 2019.

[51] H. Qiu, W. Gu, L. Wang, G. Pan, Y. Xu and Z. Wu, "Trilayer stackelberg game approach for robustly power management in community grids," *IEEE Trans. Ind. Informat.*, vol. 17, no. 6, pp. 4073-4083, Jun. 2021.

[52] M. B. Anwar and M. O'Malley, "Strategic participation of residential thermal demand response in en-ergy and capacity markets," *IEEE Trans. Smart Grid*, early access, doi: 10.1109/TSG.2021.3053639.

[53] H. Chen, L. Fu, L. Bai, T. Jiang, Y. Xue, R. Zhang, B. Chowdhury, J. Stekli and X. Li, "Distribution market-clearing and pricing considering coordination of DSOs and ISO: an EPEC approach," *IEEE Trans. Smart Grid*, early access, doi: 10.1109/TSG.2021.3061282.

[54] P. Siano and G. Mokryani, "Probabilistic assessment of the impact of wind energy integration into distribution networks," *IEEE Trans. Power Syst.*, vol. 28, no. 4, pp. 4209-4217, Nov. 2013.

[55] L. Cheng, H. Zang, Y. Xu, Z. Wei and G. Sun, "Augmented convolutional network for wind power prediction: A new recurrent architecture design with spatial-temporal image inputs," *IEEE Trans. Ind. Informat.*, Early Access, doi: 10.1109/TII.2021.3063530.

[56] F. Zhang, Y. Sun, L. Cheng, X. Li, J. H. Chow and W. Zhao, "Measurement and modeling of delays in wide-area closed-loop control systems," *IEEE Trans. Power Syst.*, vol. 30, no. 5, pp. 2426-33, Oct. 2014.

[57] H. Hui, Y. Ding, Y. Song and S. Rahman, "Modeling and control of flexible loads for frequency regulation services considering compensation of communication latency and detection error," *Appl. Energy*, vol. 15, no. 250, pp. 161-74, Apr. 2019.

[58] A. Piccolo and P. Siano, "Evaluating the impact of network investment deferral on distributed generation expansion," *IEEE Trans. Power Syst.*, vol. 24, no. 3, pp. 1559-1567, Aug. 2009.

[59] P. Siano and D. Sarno, "Assessing the benefits of residential demand response in a real time distribution energy market," *Appl. Energy*, vol. 161, pp. 533-551, Jan. 2016.

[60] P. Yu, H. Hui, H. Zhang, G. Chen and Y. Song, "District cooling system control for providing operating reserve based on safe deep reinforcement learning," *arXiv preprint arXiv*:2112.10949, Dec. 2021.

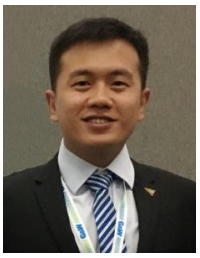

Hongxun Hui (S'17-M'20) received the B.E. and Ph.D. degrees in electrical engineering from Zhejiang University, Hangzhou, China, in 2015 and 2020, respectively. He is currently a Post-doctoral Fellow with the State Key Laboratory of Internet of Things for Smart City, University of Macau, Macau, China. From 2018 to 2019, he was a visiting student researcher at the Advanced Research Institute in Virginia Tech, and the CURENT Center in University of Tennessee. He was elected in the 1st batch of the Academic Rising Star Program for Ph.D. students in Zhejiang University in 2018. His research interests include power system stability analysis, microgrid optimization, and control of flexible resources in smart grid. In these fields, he has authored 1 international book and more than 30 journal papers, including one ESI Highly Cited Paper.

Pierluigi Siano (M'09-SM'14) received the M.Sc. degree in electronic engineering and the Ph.D. degree in information and electrical engineering from the University of Salerno, Salerno, Italy, in 2001 and 2006, respectively. He is a Professor and Scientific Director of the Smart Grids and Smart Cities Laboratory with the Department of Management & Innovation Systems, University of Salerno. Since 2021 he has been Distinguished Visiting Professor in the Department of Electrical & Electronic Engineering Science, University of Johannesburg. His research activities are centered on demand response, on the integration of distributed energy resources in smart grids and on planning and management of power systems. In these research fields, he has co-authored more than 370 articles published in international journals that received in Scopus more than 12700 citations with an H-index equal to 55. In 2019, 2020 and 2021 he has been awarded as Highly cited Researcher in Engineering by Web of Science Group. He has been the Chair of the IES TC on Smart Grids. He is Editor for Power & Energy Society Section of IEEE Access, IEEE Transactions on Power Systems, IEEE Transactions on Industrial Informatics, IEEE Transactions on Industrial Electronics, and IEEE Systems.

Yi Ding (M'12) received the bachelor degree in electrical engineering from Shanghai Jiaotong University, Shanghai, China in 2000, and the Ph.D. degree from Nanyang Technological University, Singapore in 2007. He is currently a Professor with the College of Electrical Engineering, Zhejiang University, Hangzhou, China. His research interests include power systems reliability and performance analysis incorporating renewable energy resources, and engineering systems reliability modeling and optimization.

Peipei Yu (S'21) received the B.S. and M.S. degrees in mathematics from Zhejiang University, Zhejiang, China, in 2016 and 2019, respectively. She is currently working toward the Ph.D. degree at University of Macau, Macau, China. She was the winner of the First Prize and the only Best Innovation Award at the national competition on artificial intelligence (AI) application in power dispatching in 2021. Her research interests include Internet of Things for smart energy, demand response and reinforcement learning control.

Yonghua Song (F'08) received the B.E. and Ph.D. degrees from Chengdu University of Science and Technology, Chengdu, China, and the China Electric Power Research Institute, Beijing, China, in 1984 and 1989, respectively, all in electrical engineering. He was awarded DSc by Brunel University in 2002, Honorary DEng by University of Bath in 2014 and Honorary DSc by University of Edinburgh in 2019. From 1989 to 1991, he was a Post-Doctoral Fellow at Tsinghua University, Beijing. He then held various positions at Bristol University, Bristol, U.K.; Bath University, Bath, U.K.; and John Moores University, Liverpool, U.K., from 1991 to 1996. In 1997, he was a Professor of Power Systems at Brunel University, where he was a Pro-Vice Chancellor for Graduate Studies since 2004. In 2007, he took up a Pro-Vice Chancellorship and Professorship of Electrical Engineering at the University of Liverpool, Liverpool. In 2009, he joined Tsinghua University as a Professor of Electrical Engineering and an Assistant President and the Deputy Director of the Laboratory of Low-Carbon Energy. During 2012 to 2017, he worked as the Executive Vice President of Zhejiang University, as well as Founding Dean of the International Campus and Professor of Electrical Engineering and Higher Education of the University. Since 2018, he became Rector of the University of Macau and the director of the State Key Laboratory of Internet of Things for Smart City. His current research interests include smart grid, electricity economics, and operation and control of power systems. Prof. Song was elected as the Vice-President of Chinese Society for Electrical Engineering (CSEE) and appointed as the Chairman of the International Affairs Committee of the CSEE in 2009. In 2004, he was elected as a Fellow of the Royal Academy of Engineering, U.K. In 2019, he was elected as a Foreign Member of the Academia Europaea.

Hongcai Zhang (S'14-M'18) received the B.S. and Ph.D. degrees in electrical engineering from Tsinghua University, Beijing, China, in 2013 and 2018, respectively. He is currently an Assistant Professor with the State Key Laboratory of Internet of Things for Smart City and Department of Electrical and Computer Engineering, University of Macau, Macau, China. In 2018-2019, he was a postdoctoral scholar with the Energy, Controls, and Applications Lab at University of California, Berkeley, where he also worked as a visiting student researcher in 2016. His current research interests include Internet of Things for smart energy, optimal operation and optimization of power and transportation systems, and grid integration of distributed energy resources.

Ningyi Dai (S'05-M'08-SM'15) received the B.Sc. degree in Electrical Engineering from Southeast University, Nanjing, China, in 2001, and the M.Sc. and Ph.D. degrees in Electrical and Electronics Engineering from the Faculty of Science and Technology, University of Macau, Macau, China, in 2004 and 2007, respectively. She is currently an Associate Professor with the Department of Electrical and Computer Engineering and State Key Laboratory of Internet of Things for Smart City, University of Macau, Macau, China. She has authored or co-authored more than 70 technical journals and conference papers in power systems and power electronics. Her current research interests include the application of power electronics in power systems, renewable energy integration, and integrated energy system. She was a corecipient of the Macao Science and Technology Invention Award in 2012 and 2018.